Chaotic Modeling and Simulation (CMSIM) 2: 147–157, 2017

On an extension of the nonlinear feedback loop within a nine-dimensional Lorenz model

Bo-Wen Shen

Department of Mathematics and Statistics, San Diego State University
E-mail: bshen@mail.sdsu.edu; bowen.shen@gmail.com

Abstract. In a recent study, a seven-dimensional Lorenz Model (7DLM) was derived based on an extension of the nonlinear feedback loop within the five-dimensional LM (5DLM). An analysis of Lyapunov exponents indicated that the 7DLM requires a much larger critical value for the Rayleigh parameter (rc $\sim$ 116.9) for the onset of chaos as compared to the rc of 24.74 for the original three-dimensional (3D) LM and the rc of 42.9 for the 5DLM. To assure that the 7DLM is more stable than the 3DLM and 5DLM, analytical solutions of the critical points for the 7DLM were obtained and a linear stability analysis near the critical point solutions was performed using various values of the Rayleigh parameter ($40 \leq r \leq 195$) and the Prandtl number ($5 \leq \sigma \leq 25$). In derivations of the 7DLM, potential temperature is represented by the primary, secondary, and tertiary modes, while the streamfunction is represented only by the primary mode. I also further derive a nine-dimensional LM (9DLM) by extending the 7DLM with secondary and tertiary modes for the streamfunction. By comparing the 9DLM with the 7DLM, the negative nonlinear feedback associated with the tertiary temperature modes, as first identified in the 7DLM, is determined to play a dominant role in stabilizing solutions, while the secondary and tertiary modes for the streamfunction produce additional heating terms that slightly destabilize solutions. The critical value of the Rayleigh parameter for the 9DLM is determined to be 102.9, smaller than that of the 7DLM but still much larger than those within the 3DLM and 5DLM. Additionally, as indicated by the strong bivariate relationship among primary, secondary, and tertiary temperature modes, hierarchical scale dependence appears in the 9DLM as well as the 7DLM. Therefore, the comparison between the 7DLM and the 9DLM suggests that using the 7DLM is effective for examining the impact of high-wavenumber modes on solutions stability.
Keywords: Lorenz model, Chaos, Predictability, Butterfly effect.

1 Introduction

Since Prof. Lorenz of MIT illustrated the sensitive dependence of solutions on initial conditions over 50 years ago [1,2], his studies have significantly changed scientific views regarding the predictability of short-term weather and long-term climate simulations [3,4]. Due to the work of Lorenz, it is now accepted

Received: 17 April 2016 / Accepted: 15 December 2016

ISSN 2241-0503

that perfect deterministic predictions are impossible and that only finite predictability can be obtained. Since the practical predictability of a model depends on the model's mathematical formulas [5], high-dimensional Lorenz models have been examined in numerous studies (e.g.,[6–8]) in order to understand the impact of additional Fourier modes on systems responses. However, earlier studies have not provided a solid answer as to whether increasing the number of modes can produce a model with better predictability. In a series of recent papers [8–11], to address the above question, a systematic approach was applied by deriving the five-dimensional (5D), six-dimensional (6D), and seven-dimensional (7D) Lorenz models (LMs). These 5D-, 6D-, and 7D-LMs were derived using new modes that can extend the nonlinear feedback loop [8] within the original 3DLM [1]. The nonlinear feedback loop is identified through an analysis of the Jacobian term ($J(\psi, \theta)$) that represents the advection of temperature perturbation (θ) by the streamfunction (ψ). To facilitate discussions, the three Fourier modes used in the 3DLM are referred to as the primary modes; the two (three) additional Fourier modes in the 5DLM (6DLM) are referred to as the secondary modes; and the new Fourier modes in the 7DLM are referred to as tertiary modes (see details in Section 2). Using these high-dimensional LMs, the following results were obtained:

1. The two additional secondary modes within the 5DLM, included to represent the temperature, are capable of providing negative nonlinear feedback for stabilizing solutions.
2. The third secondary mode within the 6DLM, added to represent the streamfunction, introduces an additional heating term that can destabilize solutions.
3. The findings in (1) and (2) support the view of Lorenz (1972) on the role of small scale processes: If the flap of a butterfly's wings can be instrumental in generating a tornado, it can equally well be instrumental in preventing a tornado.
4. The nonlinear feedback loop within the original 3DLM determines the "baseline predictability" and its extension within the 5DLM (or 6DLM) can provide nonlinear negative feedback and, thus, leads to better predictability as compared to the "baseline predictability" provided by the 3DLM.
5. The coupling of a new parameterization with nonlinear terms may change the quasi-equilibrium state. The coupling of a smoothing term (i.e., averaging term) with nonlinear terms may have a similar effect.
6. Further extension of the nonlinear feedback loop within the 7DLM leads to a much larger critical value for the Rayleigh parameter (rc 116.9) for the onset of chaos as compared to the rc of 24.74 for the 3DLM and the rc of 42.9 for the 5DLM.
7. As indicated by the high Pearson correlation coefficients between the primary and secondary modes and between the secondary and tertiary modes, 0.988 and 0.998, respectively, hierarchical scale dependence appears within the chaotic solutions of the 7DLM.

The above findings suggest that an improved degree of nonlinearity within a real-world, high-resolution model may stabilize solutions, leading to improved

predictability [12,13]; and that heating effects associated with excessive precipitation may destabilize solutions, thereby increasing the sensitivity of simulations to small perturbations.

While the 3DLM displays the sensitive dependence of solutions on the initial conditions, the 7DLM reveals the hierarchical scale dependence within chaotic solutions. The 7DLM was derived using the primary, secondary, and tertiary modes for temperature but only the primary mode for the streamfunction. In this study, the secondary and tertiary modes for the streamfunction are included in order to derive a nine-dimensional LM (9DLM) for comparing the impact of the additional modes on solution stability to the impact of the extended nonlinear feedback loop within the 7DLM. Section 2 discusses the derivations of the 9DLM and its relationship to the 7DLM. Results from both the 7DLM and 9DLM are presented in Section 3. A conclusion is provided at the end.

2 Seven- and Nine-dimensional Lorenz Models

In this section, I first introduce the nine-dimensional Lorenz Model (9DLM), discuss how to simplify the 9DLM to the 7DLM [11], and then compare the 7DLM and 9DLM with the 5DLM in order to illustrate the major role of the extended nonlinear feedback loop within the system solutions. By using Fourier modes to represent the streamfunction and temperature, the 3DLM and higher-dimensional LMs can be derived from the governing equations for the two-dimensional Rayleigh Benard convection (e.g., [1,14]; Equations 1-2 in [11]). To obtain the 9DLM, the following nine Fourier modes are utilized:

$$M_1 = \sqrt{2}sin(lx)sin(mz), M_2 = \sqrt{2}cos(lx)sin(mz), M_3 = sin(2mz), \quad (1)$$

$$M_4 = \sqrt{2}sin(lx)sin(3mz), M_5 = \sqrt{2}cos(lx)sin(3mz), M_6 = sin(4mz), \quad (2)$$

$$M_7 = \sqrt{2}sin(lx)sin(5mz), M_8 = \sqrt{2}cos(lx)sin(5mz), M_9 = sin(6mz). \quad (3)$$

Here l and m are defined as $\pi a/H$ and π/H, representing the horizontal and vertical wavenumbers, respectively; a is a ratio of the vertical scale of the convection cell to its horizontal scale (i.e., $a = l/m$). H is the domain height, and $2H/a$ represents the domain width.

With the modes in Eqs. (1-3), the streamfunction, ψ, and the temperature perturbation, θ, can be represented as:

$$\psi = C_1\bigg(XM_1 + X_1M_4 + X_2M_7\bigg), \quad (4)$$

$$\theta = C_2\bigg(YM_2 - ZM_3 + Y_1M_5 - Z_1M_6 + Y_2M_8 - Z_2M_9\bigg). \quad (5)$$

C_1 and C_2 are constants and are defined in Eq. (9) of Shen (2014) [8]. While the modes in Eq. (1) were used to derive the 3DLM [1], additional modes in Eq. (2) were included in order to derive the 6DLM [10]. New modes in

Eq. (3) are added in order to derive the 9DLM. The modes in Eqs. (1-3) are referred to as the primary, secondary, and tertiary modes, respectively. The three modes (M_1, M_4, M_7) in Eq. (4) are called streamfunction modes, and the six modes ($M_2, M_3, M_5, M_6, M_8, M_9$) in Eq. (5) are called temperature modes. ($X, Y, Z, X_1, Y_1, Z_1, X_2, Y_2, Z_2$) represent the amplitudes of the Fourier modes (M_1-M_9), respectively. Based on the analysis of the Jacobian term ($J(\psi, \theta)$), the secondary and tertiary temperature modes ($M_5 - M_6$ and $M_8 - M_9$) are selected in order to extend the nonlinear feedback loop of the 3DLM. More details on the selection of the secondary and tertiary modes can be found in the supplemental materials of [10]. Using Eqs. (1-5), the partial differential equations for the two-dimensional Rayleigh-Benard convection can be transformed into a set of ordinary differential equations, as follows:

$$\frac{dX}{d\tau} = -\sigma X + \sigma Y, \tag{6}$$

$$\frac{dY}{d\tau} = -XZ + X_1 Z - 2X_1 Z_1 + 2X_2 Z_1 - 3X_2 Z_2 + rX - Y, \tag{7}$$

$$\frac{dZ}{d\tau} = XY - XY_1 - X_1 Y - X_1 Y_2 - X_2 Y_1 - bZ, \tag{8}$$

$$\frac{dX_1}{d\tau} = -d_o \sigma X_1 + \frac{\sigma}{d_o} Y_1, \tag{9}$$

$$\frac{dY_1}{d\tau} = XZ - 2XZ_1 - 3X_1 Z_2 + X_2 Z + rX_1 - d_o Y_1, \tag{10}$$

$$\frac{dZ_1}{d\tau} = 2XY_1 - 2XY_2 + 2X_1 Y - 2X_2 Y - 4bZ_1, \tag{11}$$

$$\frac{dX_2}{d\tau} = -d_1 \sigma X_2 + \frac{\sigma}{d_1} Y_2, \tag{12}$$

$$\frac{dY_2}{d\tau} = 2XZ_1 - 3XZ_2 + X_1 Z + rX_2 - d_1 Y_2, \tag{13}$$

$$\frac{dZ_2}{d\tau} = 3XY_2 + 3X_1 Y_1 + 3X_2 Y - 9bZ_2. \tag{14}$$

Here, $\tau = \kappa(1 + a^2)(\pi/H)^2 t$ (dimensionless time), $\sigma = \nu/\kappa$ (the Prandtl number), $r = R_a/R_c$ (the normalized Rayleigh number or the heating parameter), $b = 4/(1 + a^2)$, $d_o = (9 + a^2)/(1 + a^2)$, and $d_1 = (25 + a^2)/(1 + a^2)$. ν and κ denote the kinematic viscosity and the thermal conductivity, respectively. R_a is the Rayleigh number and R_c is its critical value for the free-slip Rayleigh-Benard problem. An eight-dimensional LM (8DLM) can be obtained by neglecting Eq. (12) and terms that involve X_2 in Eqs. (6-14). The 7DLM can be obtained by neglecting Eqs. (9) and (12) and the terms that involve X_1 and X_2 in Eqs. (6-14). The 7D-, 8D- and 9D-LMs include all of the primary, secondary, and tertiary temperature modes. While the 7DLM only contains the primary streamfunction mode, the 8DLM has both the primary and secondary streamfunction modes. The 9DLM includes all of the primary and secondary and tertiary streamfunction modes.

Using the definitions of domain-averaged kinetic energy ($\overline{KE}$) and available potential energy ($\overline{APE}$) in [10], the following equations can be obtained:

$$\overline{KE} = \frac{C_o}{2}\left(X^2 + d_o X_1^2 + d_1 X_2^2\right), \tag{15}$$

$$\overline{APE} = -\frac{C_o}{2}\frac{\sigma}{r}\left(Y^2 + Z^2 + Y_1^2 + Z_1^2 + Y_2^2 + Z_2^2\right), \tag{16}$$

where $C_o = \pi^2\kappa^2(\frac{1+a^2}{a})^3$. With Eqs. (6-14) in the dissipationless limit, the time derivative of the sum of Eqs. (15) and (16) is zero (i.e., $d(KE + APE)/d\tau = 0$). Therefore, the following energy conservation law is obtained:

$$\overline{KE} + \overline{APE} = constant. \tag{17}$$

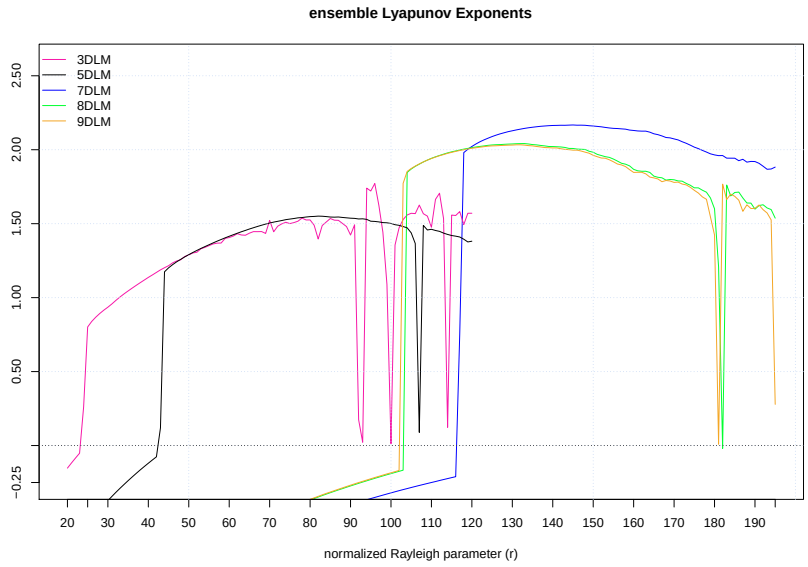

Fig. 1. The largest ensemble-averaged Lyapunov Exponents (eLEs) as a function of the forcing parameter, r, in various LMs. The figure provides results for $\triangle r$=1. The pink, black, blue, green, and orange lines display eLEs for the 3DLM, 5DLM, 7DLM, 8DLM, and 9DLM, respectively. The appearance of chaotic solutions is indicated by positive eLEs. Note that the critical value of r for the onset of chaos is between r=116 and r=117 for the 7DLM, and between r=102 and r=103 for the 9DLM. The pink and black lines are reproduced from [8].

To determine under which condition a model produces chaotic solutions, the Lyapunov exponent (LE) as a function of the Rayleigh parameter has been

used ([15]). In this and other studies conducted by myself and other collaborators ([8–11]), numerical methods for calculation of an ensemble averaged LE (eLE) are developed in order to quantitatively evaluate whether or not the system is chaotic. An eLE is determined by averaging 10,000 LEs obtained from 10,000 ensemble runs each of which produces one LE using the same model configurations but different ICs. With the exception of the heating parameter (r), the following parameters are kept as constant: $a = 1/\sqrt{2}$, $b = 8/3$, $d_o = 19/3$, $d_1 = 17$, and $\sigma = 10$. While Figure 1 displays eLEs obtained using various values of the Rayleigh parameter ($40 \leq r \leq 195$), Figures 2-3 provide scatter plots with $r = 120$ for a comparison between the 7DLM and 9DLM. Detailed discussions on the numerical methods used for calculations of the eLE and solutions can be found in [8,10].

3 Numerical Results

In this section, characteristics of the solutions for both the 7DLM and 9DLM are discussed. Figure 1 provides eLMs for the two models, as well as the 3DLM and 5DLM, for a comparison. For the 9DLM, its critical value for the Rayleigh parameter ($rc \sim 102.9$) for the onset of chaos is comparable but smaller than the rc of 116.9 for the 7DLM. Both models produce much larger critical values, as compared to the rc of 24.74 for the 3DLM and the rc of 42.9 for the 5DLM. Table 1 summarizes critical values for the models. As discussed in [11], when the tertiary temperature modes were included within the 7DLM, the extension of the nonlinear feedback loop produced negative nonlinear feedback to stabilize solutions. As the 9DLM is a superset of the 7DLM, results with a comparable rc may indicate that the negative nonlinear feedback associated with the tertiary temperature modes also plays a major role in stabilizing the solutions. On the other hand, when additional secondary and tertiary streamfunction modes are included in order to extend the 7DLM to the 9DLM, a slightly smaller r_c for the 9DLM may suggest the impact of destabilization by the two streamfunction modes that produce additional heating terms. A similar result was previously obtained from a comparison between the 5DLM and 6DLM, since the 5DLM with a larger rc only contains one heating term while the 6DLM with a smaller rc has two heating terms (see also Table 1). Further analysis between the 7DLM and 9DLM is provided below.

For the 7DLM, in addition to the negative nonlinear feedback associated with the extended nonlinear feedback loop, hierarchical scale dependence is another unique characteristic of the solutions. Hierarchical scale dependence was first shown with the high correlation coefficients for two modes among the primary, secondary, and tertiary temperature modes [11]. In the following, I will discuss whether hierarchical scale dependence also appears in the 9DLM that contains additional streamfunction modes. To achieve the goal effectively, in Figure 2, I begin my discussions with a matrix of scatter plots for the 7DLM. The plots are generated from the numerical results of Shen (2016) [11] using numerical packages in R ([16]). The scatter-plot matrix displays a bivariate relationship amongst all of the seven variables, including X, Y, Z, Y_1, Z_1, Y_2, and Z_2, as shown in the diagonal cells. Each of the cells below the principal

Table 1. The characteristics of various Lorenz models. Values for r_c and r_c^1 are determined based on the eLE analyses and the linear stability analyses [8,11] , respectively. The "Equations" column provides a list of the equations used in each specific Lorenz model. The "Heating terms" column indicates heating terms within the corresponding LM. The "Models" list selected modes for the LM. Note that the 3DLM, 5DLM, and 7DLM only have one heating term.

Model	r_c	r_c^1	Equations	Heating terms	Modes
3DLM	23.7	24.74	Eqs. (15)–(17) in [8]	rX	M_1-M_3
5DLM	42.9	45.94	Eqs. (10)–(14) in [8]	rX	M_1-M_3, M_5-M_6
6DLM	41.1	N/A	Eqs. (8)–(13) in [9]	rX, rX_1	M_1-M_6
7DLM	116.9	160.3	Eqs. (11)–(17) in [11]	rX	M_1-M_3, M_5-M_6, M_8-M_9
8DLM	103.4	N/A	Eqs. (6)–(14) with no X_2	rX, rX_1	M_1-M_6,M_8-M_9
9DLM	102.9	N/A	Eqs. (6)–(14)	rX, rX_1, rX_2	M_1-M_9

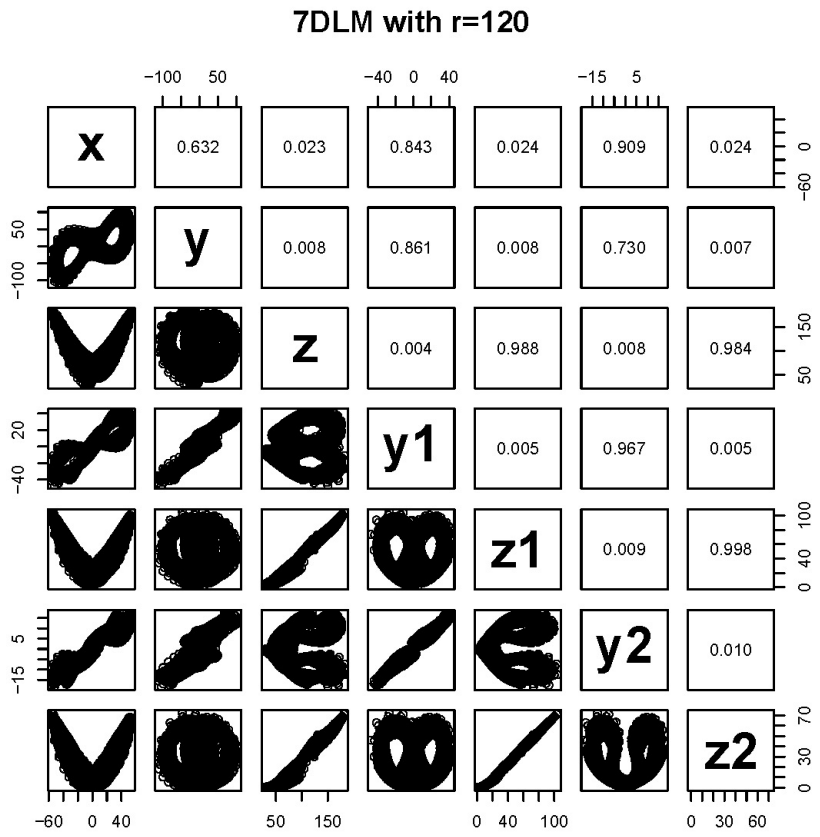

Fig. 2. A matrix of scatter plots for the 7DLM with its seven variables, as listed in the principal diagonal. r and σ are 120 and 10, respectively. Each of the cells above (below) the diagonal shows a PCC (scatter plot) between the two variables. Scale dependence is indicated by high PCCs, as well as the linear relationship, in scatter plots.

diagonal provides a scatter plot of two variables at the row and column interaction of the two variables. For example, the second cell in the first column is a scatter plot of X (horizontal axis) and Y (vertical axis). Each of the cells above the diagonal provides the Pearson correlation coefficient (PCC) of two variables at the row and column intersection of the two variables. For example, the second cell in the first row indicates the PCC between X and Y, denoted by PCC(X,Y). From the cells above the diagonal in Figure 2, high PCCs can be found in two variables among Y, Y_1, and Y_2 and among Z, Z_1, and Z_2. The PCC(Z, Z_1), PCC(Z_1, Z_2), and PCC(Z, Z_2) are 0.988, 0.998, and 0.984, respectively, suggesting the scale dependence. Additionally, since the PCC of the primary and tertiary modes (PCC(Z, Z_2)) is smaller than the PCC of the primary and secondary modes (PCC(Z, Z_1)) and the PCC of the secondary and tertiary modes (PCC(Z_1, Z_2)), the results indicate the appearance of hierarchical scale dependence. The PCC(Y, Y_1), PCC(Y_1, Y_2), and PCC(Y, Y_2) are 0.861, 0.967, and 0.730, respectively, which also indicates hierarchical scale dependence. A strong linear relationship amongst the above variables is clearly shown by scatter plots in the cells below the diagonal.

Figure 3 displays the scatter-plot matrix for the 9DLM, which includes the additional variables of X_1 and X_2. For the PCCs, PCC(Z, Z_1), PCC(Z_1, Z_2) and PCC(Z, Z_2) are 0.979, 0.998, and 0.972, respectively, slightly smaller than those in the 7DLM. Similar scatter plots are also obtained with the exception of the cells that involve additional modes (X_1 and X_2). Therefore, hierarchical scale dependence (for the temperature modes) also appears within the 9DLM. Additionally, a linear relationship appears in each pair of the primary, secondary, and tertiary streamfunction modes (e.g., X, X_1, and X_2). However, the PCC(X, X_2) of 0.905 is slightly greater than the PCC (X, X_1) of 0.901. In my future work, I will verify whether or not hierarchical scale dependence appears amongst the streamfunction modes. Figure 3 also displays a strong linear relationship between X_1 and Y_1 with a PCC of 0.973, and between X_2 and Y_2 with a PCC of 0.996. Therefore, statistically, the following regression models can be employed to relate X_1 (X_2) to Y_1 (Y_2):

$$X_1 \sim \alpha_1 + \beta_1 Y_1, \tag{18}$$

$$X_2 \sim \alpha_2 + \beta_1 Y_2, \tag{19}$$

where (α_1, β_1)=(-9.87×10^{-4}, 2.36×10^{-2}) and (α_2, β_2)=(-7.5×10^{-6}, 3.43×10^{-3}). Equations (18-19) can be further simplified into the following: $rX_1 \sim r\beta_1 Y_1$ and $rX_2 \sim r\beta_2 Y_2$ that act as a forcing term in Eqs. (10) and (13), respectively. Based on an analysis of the coefficients in Eqs. (18-19), as well as the scale analysis in Eqs. (9) and (12), X_1 and X_2 are statistically much smaller than Y_1 and Y_2, respectively. Therefore, the inclusion of X_1 and X_2 may slightly destabilize the solutions. In summary, the 9DLM has a similar rc as compared to the 7DLM. While the tertiary temperature modes of the 9DLM extend the nonlinear feedback loop of the 5DLM, providing negative nonlinear feedback for stabilizing solutions, the secondary and tertiary streamfunction modes introduce additional heating terms that slightly destabilize solutions. The latter was not included within the 7DLM.

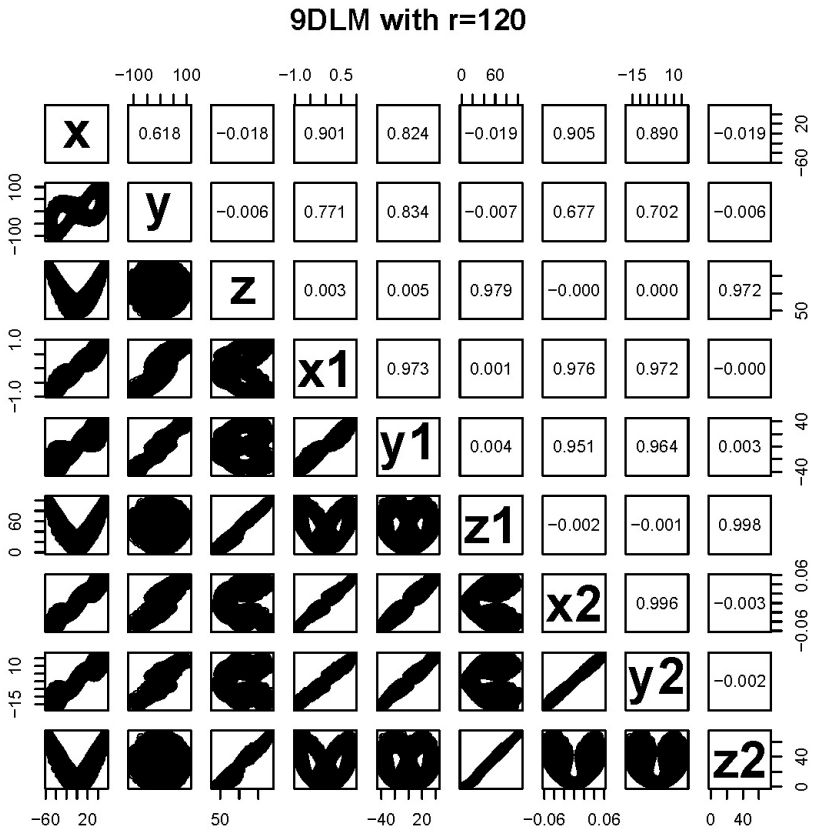

Fig. 3. The same as for Figure 2 but for the 9DLM with its nine variables, as listed in the principal diagonal.

4 Conclusions

Over 50 years ago, Prof. Lorenz discovered the sensitive dependence of numerical solutions on initial conditions and changed scientific views regarding the predictability of weather and climate simulations. In recent studies and in this study, I reported the role of negative nonlinear feedback in stabilizing solutions and the appearance of hierarchical scale dependence within chaotic solutions of the 7DLM and 9DLM. The negative nonlinear feedback, associated with the extension of the nonlinear feedback loop of the 5DLM [11], is enabled by the tertiary temperature modes (i.e., M_8 and M_9) in both the 7DLM and 9DLM. In comparison with the extended feedback loop, additional heating terms of the 9DLM, associated with the two additional modes (i.e., M_4 and M_7 as the secondary and tertiary streamfunction modes), can destabilize solutions. Based on the analysis, responses associated with the additional streamfunction modes are weaker than those associated with the tertiary temperature modes.

As compared to the rc of 116.9 for the 7DLM, the 9DLM has a comparable but slightly smaller critical value of the Rayleigh parameter ($rc \sim 102.9$) for the onset of chaos. Both models produce much larger values of rc, as compared to the rc of 24.74 for the 3DLM and the rc of 42.9 for the 5DLM. Therefore, I suggest that examining the impact of additional modes on solution stability by extending the nonlinear feedback loop of the 7DLM is effective. Currently, a new 9DLM is being derived and examined by excluding the secondary and tertiary streamfunction modes and by including two additional higher wavenumber temperature modes.

Acknowledgements

I thank X. Zeng, R. Pielke Sr., and Chii-Dean (Joey) Lin for valuable discussions, and E. K. Yoo for her help in the derivations and verification of the seven- and nine-dimensional Lorenz models. I am grateful for support from the College of Science at San Diego State University and the NASA Advanced Information System Technology (AIST) Program. Resources supporting this work were provided by the NASA High-End Computing (HEC) program and the NASA Advanced Supercomputing division at Ames Research Center.

References

1. Lorenz, E.: Deterministic nonperiodic flow, J. Atmos. Sci., 20, 130–141, 1963.
2. Lorenz, E.: Predictability: does the flap of a butterfly's wings in Brazil set off a tornado in Texas?, in: American Association for the Advancement of Science, 139th Meeting, 29 December 1972, Boston, Mass., AAAS Section on Environmental Sciences, New Approaches to Global Weather, GARP, available at: http://eaps4.mit.edu/research/Lorenz/Butterfly_1972.pdf, last access: 14 December 2015, 1972.
3. IPCC: Climate Change 2007: The Physical Science Basis, in: Contribution of Working Group I to the Fourth Assessment Report of the Intergovernmental Panel on Climate Change, edited by: Solomon, S., Qin, D., Manning, M., Chen, Z., Marquis, M., Averyt, K. B., Tignor, M., and Miller, H. L., Cambridge University Press, Cambridge, UK and New York, NY, USA, 996 pp.
4. Pielke, R.: The Real Butterfly Effect, available at: http://pielkeclimatesci.wordpress.com/2008/04/29/the-real-butterfly-effect/, last access: 14 December 2015, 2008.
5. Lorenz, E.: The predictability of hydrodynamic flow. Transactions of The New York Academy of Sciences, Ser. II, 25(4), 409432, 1963b.
6. Curry, J. H., Herring, J. R., Loncaric, J., and Orszag, S. A.: Order and disorder in two- and three-dimensional Benard convection, J. Fluid. Mech., 147, 1–38, 1984.
7. Roy, D. and Musielak, Z. E.: Generalized Lorenz models and their routes to chaos, I. Energy-conserving vertical mode truncations, Chaos Soliton. Fract., 32, 1038–1052, 2007.
8. Shen, B.-W.: Nonlinear feedback in a five-dimensional Lorenz model, J. Atmos. Sci., 71, 1701–1723, doi:10.1175/JAS-D-13-0223.1, 2014.
9. Shen, B.-W.: Parameterization of Negative Nonlinear Feedback using a Five-dimensional Lorenz Model, Fractal Geometry and Nonlinear Analysis in Medicine and Biology, 1, 33–41, doi:10.15761/FGNAMB.1000109, 2015a.

10. Shen, B.-W.: Nonlinear feedback in a six dimensional Lorenz model: impact of an additional heating term, Nonlin. Processes Geophys., 22, 749-764, doi:10.5194/npg-22-749-2015, 2015b.
11. Shen, B.-W.: Hierarchical scale dependence associated with the extension of the nonlinear feedback loop in a seven-dimensional Lorenz model. Nonlin. Processes Geophys., 23, 189-203, doi:10.5194/npg-23-189-2016, 2016.
12. Shen, B.-W., Atlas, R., Reale, O., Lin, S.-J., Chern, J.-D., Chang, J., Henze, C., and Li, J.-L.: Hurricane forecasts with a global mesoscale-resolving model: Preliminary results with Hurricane Katrina (2005), Geophys. Res. Lett., 33, L13813, doi:10.1029/2006GL026143, 2006.
13. Shen, B. W., DeMaria, M., Li, J.-L. F., and Cheung, S.: Genesis of hurricane Sandy (2012) simulated with a global mesoscale model, Geophys. Res. Lett., 40, 4944–4950, doi:10.1002/grl.50934, 2013.
14. Saltzman, B.: Finite amplitude free convection as an initial value problem, J. Atmos. Sci., 19, 329–341, 1962.
15. Wolf, A., Swift, J. B., Swinney, H. L., and Vastano, J. A.: Determining Lyapunov exponents from a time series, Physica, 16, 285–317, 1985.
16. Kabacoff, R. I: R in Action: Data Analysis and Graphics with R. Manning Publications 472 pp, 2011.